FABRICATION AND MEASUREMENTS OF SURFACE-ETCHED-GRATING DISTRIBUTED BRAGG REFLECTOR LASER

BY

UGUEN CHOI

THESIS

Submitted in partial fulfillment of the requirements
for the degree of Master of Science in Electrical and Computer Engineering
in the Graduate College of the
University of Illinois at Urbana-Champaign, 2012

Urbana, Illinois

Adviser:

Professor James J. Coleman

ABSTRACT

A laser diode emits light at a specific wavelength band and can be used in specific applications depending on its wavelength. However, the bandwidth of the laser gain is relatively broad, so a distributed Bragg reflector (DBR) laser is used to make a narrow linewidth laser. The thesis discusses semiconductor lasers that use surface-etched DBR along with the physics of both the semiconductor and the DBR laser. The topics addressed are the fabrication of the broad area laser, ridge waveguide laser, and distributed Bragg reflector broad area and ridge waveguide laser. The thesis reports on the characterization of the laser with different measurements and the physics behind each measurement.

ACKNOWLEDGMENTS

I first thank my adviser, Professor Jim Coleman, for introducing me to the field of optoelectronics and giving me the opportunity to study the field. He supports my work with patient and proper guidance that has helped me arrive at this stage of my study. I really appreciate him not kicking me out with my stupid and crazy ideas. I also thank my lab mates Neville Dias, Uttam Reddy, Jonathan Young, Jeong Dong Kim, Joseph Zimmerman, Bryan Woodard, Chunhua Wang, and Yun Lu for helping me with my work; we have enjoyed working together. I would also like to thank my parents as well as my family, who endlessly support my study.

TABLE OF CONTENTS

CHAPTER 1. INTRODUCTION

Today, we enjoy high speed internet, and large capacity portable discs such as Blu-ray and digital video disk (DVD). Behind these convenient and beneficial technologies, there is a small device called a semiconductor laser. Many people think of a laser as the large and complicated device that they see in science fiction movies, and not related to their lives. However, lasers already pervade our society with many different technologies. For example, the Internet can network the world due to 1550nm indium phosphide lasers with efficient light emission for fiber optic communication. Other examples are the laser printer, surgical laser, laser pointer, and laser gun for speeding check.

Early laser research concentrated on gas and solid-state non-semiconductor lasers. Since then, due to their high optical gain, compact semiconductor lasers have keyed today's advanced technology. Another advantage of the semiconductor laser is that, in contrast to the gas laser, it does not require external alignment for high precision because of its mechanical structure. A semiconductor laser is made by a cleaved edge where the refractive index difference between GaAs and air works as a partial mirror that gives proper feedback for lasing to occur.

1.1 History of the semiconductor laser

The first well-organized theory of semiconductor lasing was suggested by Bernard and Duraffourg in 1961 [1]. They showed the condition for gain greater than loss to emit light. In 1962, four groups reported successful fabrication of a semiconductor laser [2]-[5]. These lasers operated in pulsed mode, and had poor efficiency that makes light emission happen only at high current density (19000A/cm^2) and cryogenic temperature. In 1965, Pilkuhn and Rupprecht from IBM reported the first CW operating semiconductor laser diode operating at liquid nitrogen temperature [6].

However, lasing in a simple P-N junction is not efficient enough for a useful semiconductor laser, so Kroemer proposed the heterojunction laser in 1963 [7]. A heterojunction is a structure in which two different materials form a junction. The layers should have different band-gap energy to confine the carriers for population inversion, and should have lower refractive index in order to confine the light. Therefore, the heterojunction can automatically behave as a waveguide [8]. In 1969, Hayashi et al. reported the first room-temperature operating heterojunction laser with GaAs and AlGaAs structure [9]. However, just a single heterojunction is not enough, so people started to make a double heterojunction for better electrical and optical confinement [10]. Double heterostructure lasers eventually operated in CW room-temperature conditions, but this was not the limit of the laser structure. In 1973, Panish, et al., of Bell Laboratories first proposed the separate confinement heterostructure that had carrier and optical confinement separately by putting higher band gap material layers outside of regular double heterostucture [11]. In 1974, Dingle et al. at Bell Laboratories successfully fabricated the first quantum well laser [12].

The low threshold current of the semiconductor laser has been achieved with heterostructure, but it is not enough for precise wavelength applications that require a small bandwidth such as optical communication even though it is more selective in emitted wavelength than the light-emitting diode. Therefore, research has started to focus on how to get a small bandwidth characteristic in the semiconductor laser, and devices like the distributed feedback (DFB) laser and distributed Bragg reflector (DBR) laser have been developed. The first semiconductor DFB laser was reported by Scifres et al. in 1974 [13]. They used a single heterostructure with GaAs and AlGaAs with wavelength from 843nm to 856nm. Reinhart et al.

reported the first DBR laser with GaAs and AlGaAs in 1975 using both single and double heterostructure [14].

1.2 Basics of semiconductor laser

Laser is an acronym for “light amplification by stimulated emission of radiation”. From this phrase, we can infer what is needed for the semiconductor device to work as a laser. First, we need amplification. Amplification can be obtained by a gain medium with direct band-gap material for a semiconductor laser such as GaAs. Direct band-gap material is essential for this gain medium because it can emit a photon with the least energy as well as the highest overlap between the conduction band and valence band. However, to emit the photon in indirect band-gap material, we need to satisfy two conditions: conservation of energy and conservation of momentum. Even though we apply enough energy and engineer the structure to satisfy the above condition, a photon will not be emitted because the probability of recombining as stimulated emission is very low. Another mechanism for amplification is pumping the gain medium electronically. Provided with electrons and holes, the gain medium can recombine two carriers with its band-gap that decides the wavelength of the emitted light. The carrier injection should be sufficient to achieve population inversion, which is the preponderance of electrons in conduction bands and of holes in valence band. The last mechanism for amplification is optical feedback (a resonator). Two mirrors that reflect the emitted light back into the cavity for amplification are required to get high gain. For a semiconductor laser, two mirrors can be formed by a cleaved edge. Due to the crystal characteristic of a semiconductor, it can be cleaved with minimal defects on the edge, and the refractive index difference between the gain medium and air forms a natural mirror that forms a gain medium as a resonant cavity [15].

The other thing that we need is stimulated emission. There are two types of light emission in a semiconductor laser. One is spontaneous emission and the other is stimulated emission. Spontaneous emission, also called radiative recombination, is when an electron in the conduction band recombines with a hole in the valence band, emitting a photon that corresponds with the energy gap of the material. In stimulated emission, a photon arrives to the electron and hole pair, and forces the electron and hole to recombine and emit a photon with exactly the same phase and energy as the arriving photon. Figure 1.1 illustrates the two kinds of emission.

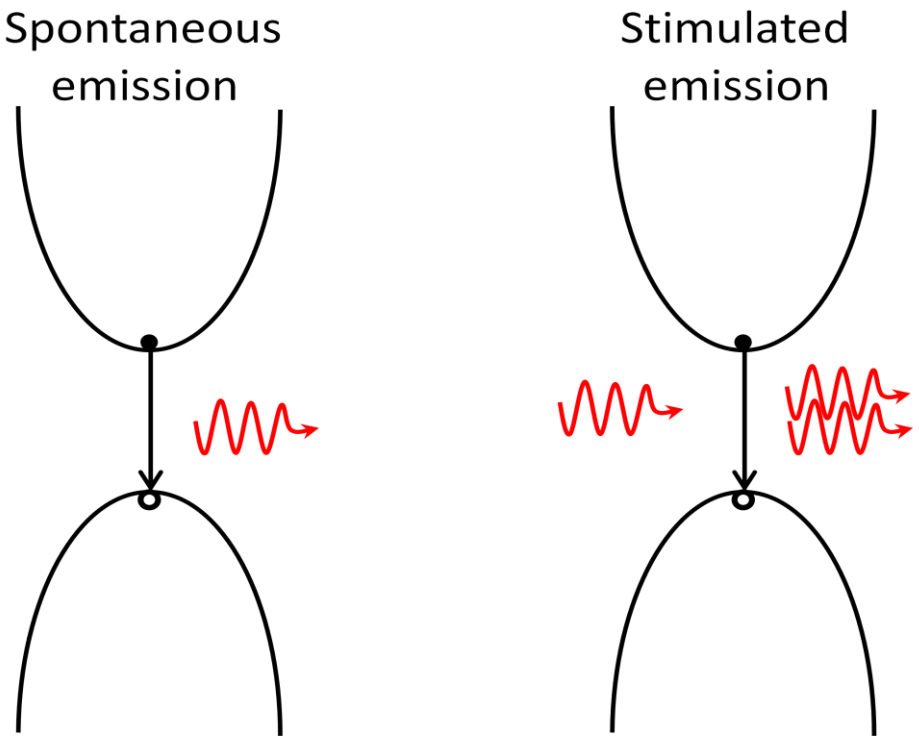

Fig 1.1 Spontaneous emission and stimulated emission

However, the gain medium, electron and hole injection, and resonator alone will not necessarily lase because there is absorption of the material, α_i, and some mirror loss, α_m. Absorption of the material is related to defects or carriers in the epi-layer growth or substrate itself, and mirror loss is related to the reflectivity of facets, R_1 and R_2, and the length of the cavity, L. (See Figure 1.2.)

$$g_{th} = \alpha_m + \alpha_i \tag{1.1}$$

$$\alpha_m = \frac{1}{2L}\ln\left(\frac{1}{R_1 R_2}\right) \tag{1.2}$$

Therefore, the laser should have higher gain than threshold gain, g_{th}, which is just the combination of two losses, and I will talk about the condition and the equation of the lasing.

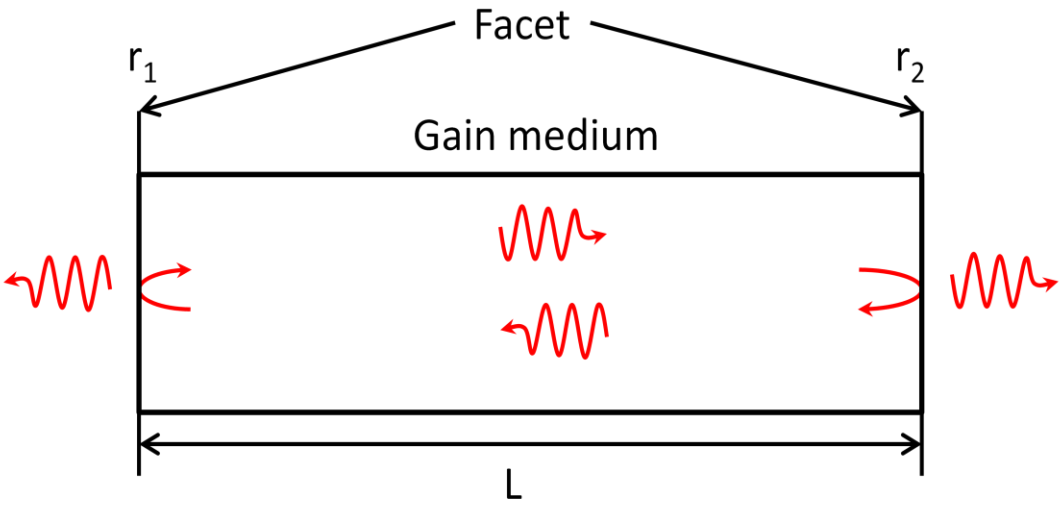

Fig 1.2 Fabry-Perot laser schematics

Equation (1.3) expresses the light as a standing wave pattern in the cavity. The condition of this equation is based on the round trip of the light that forms the resonance condition within the cavity, and we can assume that the light can be expressed as a standing wave inside the cavity [16]. Therefore, we can write

$$r_1 r_2 e^{i2kL+(G-\alpha)L} = 1 \tag{1.3}$$

$$k = \frac{2\pi n}{\lambda} \tag{1.4}$$

where r_1 and r_2 are the reflection coefficients of the mirrors, k is the propagation constant, L is the cavity length, G-α is the net gain of the cavity, n is the refractive index of the semiconductor,

and λ is the emitted wavelength. However, the standing wave pattern requires constructive interference to emit the light with maximum efficiency, so the equation should be

$$2kL = 2m\pi \tag{1.5}$$

Therefore, mathematically, the light wave will not decay or suffer destructive interference. From the equation above, we can get the equation below which we called the Fabry-Perot resonance spectrum:

$$\nu_m = \frac{mc}{2nL} \tag{1.6}$$

where ν_m is the frequency of the resonator, and *m* is an integer except 0. From this equation, we can figure out the mode spacing between two different modes as the equation below when we ignore the dispersion relation; emitted wavelength is independent of the refractive index of the material.

$$\Delta\nu = \frac{c}{2nL} \tag{1.7}$$

As the equation shows, the mode spacing is inversely proportional to the cavity length of the laser, which means that as we make the laser shorter, there will be larger mode spacing and fewer modes that overlap with the gain profile, which will be the only modes that can lase.

1.3 Dimensionally confined semiconductor laser

As mentioned in section 1.1, because of its advantages, today people use separate confinement heterostructure lasers instead of double heterostructure lasers. The laser with double heterostructure has decent performance, but the main drawback is that it cannot have a quantum well as its active layer. The quantum well laser has an easy control of its emission wavelength and low threshold current, but it is too thin to behave as an optical confinement layer. The separate confinement heterostructure laser solves problems of double heterostructure by putting a

quantum well as an active layer to get lower threshold current density and having good optical confinement. By looking at density of states (DOS), we can compare bulk and quantum well lasers, and see why the dimensionally confined laser is better.

DOS is expressed as the number of electrons or holes per unit energy per unit volume. Basically, it tells how many carriers can exist at a certain energy with a certain volume, and the derivation equations for 3D or bulk semiconductors are as follows:

$$n = \frac{2}{V}\sum_{k_x}\sum_{k_y}\sum_{k_z} f(E) \tag{1.8}$$

$$k_x = m\frac{2\pi}{L_x}, k_y = n\frac{2\pi}{L_y}, k_z = l\frac{2\pi}{L_z} \tag{1.9}$$

We first assume that we calculate with unit volume that has L_x, L_y, and L_z. V is for unit volume where it is the same as L_x*L_y*L_z, and 2 is for spin where there are always two electrons for a single state. The terms m,n,l are integers depending on the number of unit volume, so when there is only single unit volume, unit volume can be expressed as

$$(\frac{2\pi}{L_x})(\frac{2\pi}{L_y})(\frac{2\pi}{L_z}) = \frac{8\pi^3}{V} \tag{1.10}$$

By applying (1.10) to (1.8), we get

$$\frac{2}{V}\sum_{k_x}\sum_{k_y}\sum_{k_z} = \frac{2}{V}\int\frac{dk_x}{(\frac{2\pi}{L_x})}\int\frac{dk_y}{(\frac{2\pi}{L_y})}\int\frac{dk_z}{(\frac{2\pi}{L_z})} = \int\frac{d^3k}{4\pi^3} = \int\frac{k^2dk}{\pi^2} \tag{1.11}$$

Electron energy in the conduction band can be expressed as:

$$E = E_c + \frac{\hbar^2k^2}{2m_e^*} \tag{1.12}$$

Converting this expression with respect to k:

$$k = \sqrt{\frac{2m_e^*}{\hbar^2}(E - E_c)} \tag{1.13}$$

We also can express DOS as the equation below from the electron density equation where f(E) represents the Fermi-Dirac distribution.

$$n = \int dE_\rho(E) f(E) \tag{1.14}$$

$$\int \frac{k^2 dk}{\pi^2} = \int_{-\infty}^{\infty} dE \rho_e(E) \tag{1.15}$$

Therefore, we can set up (1.11) and (1.14) to be equal and plug *k* into (1.11):

$$\int \frac{k^2 dk}{\pi^2} = \int_{-\infty}^{\infty} dE \rho_e(E) \tag{1.16}$$

$$\frac{1}{3\pi^2}(\frac{2m_e^*}{\hbar^2})^{\frac{3}{2}}(E - E_c)^{\frac{3}{2}} = \int dE \rho(E) \tag{1.17}$$

Finally deriving the equation for $\rho(E)$, we get

$$\rho_e(E) = \frac{1}{2\pi^2}(\frac{2m_e^*}{\hbar^2})^{\frac{3}{2}}\sqrt{E - E_c} \qquad \text{for E > E}_c \tag{1.18}$$

DOS of holes can be derived similarly by changing a few terms and the direction of energy.

$$\rho_h(E) = \frac{1}{2\pi^2}(\frac{2m_h^*}{\hbar^2})^{\frac{3}{2}}\sqrt{E_v - E} \qquad \text{for E < E}_v \tag{1.19}$$

2D DOS, which represents the quantum well laser structure, is expressed and derived as follows:

$$n = \frac{2}{V}\sum_n \sum_{k_y} \sum_{k_z} f(E) \tag{1.20}$$

$$(\frac{2\pi}{L_x})(\frac{2\pi}{L_y}) = \frac{4\pi^2}{A} \tag{1.21}$$

$$\frac{2}{V}\sum_{k_x}\sum_{k_y}=\int\frac{dk_x}{(\frac{2\pi}{L_x})}\int\frac{dk_y}{(\frac{2\pi}{L_y})}=\int\frac{d^2k}{2\pi^2L_z}=\int\frac{kdk}{\pi L_z}=\int dE\,\rho(E) \tag{1.22}$$

From (1.21), we can get density of states for 2D structure or quantum well structure.

$$\rho_{2D}(E)=\frac{m^*}{\pi\hbar^2L_z}\sum_n H(E-E_n) \tag{1.23}$$

Here, $\sum_n H(E-E_n)$ is Heaviside step function; when E is greater than E_n, it is 1; otherwise, it is 0. Therefore, when we draw 2D DOS, it looks like a step-function as shown in Figure 1.3.

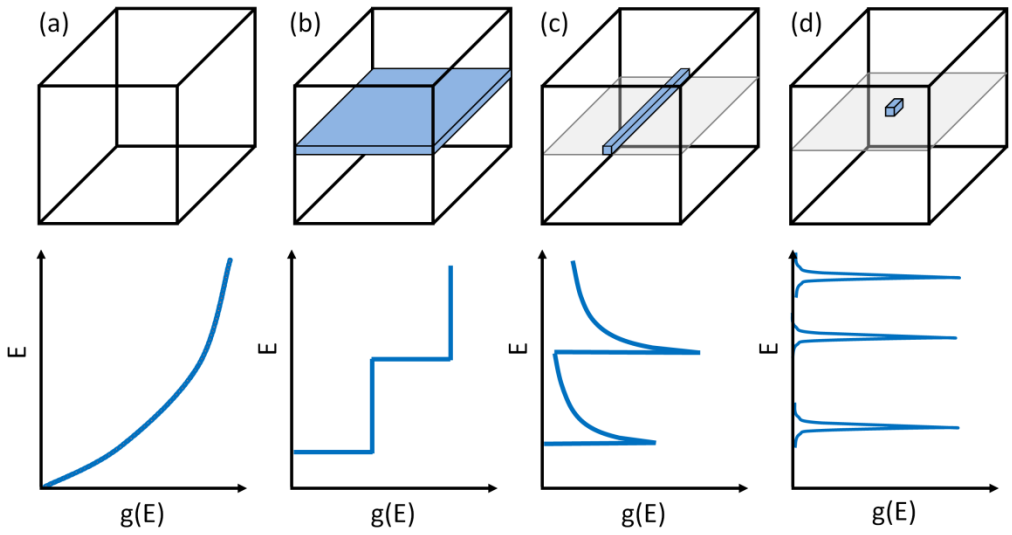

Fig 1.3 Density of states for different dimensional confinement

With DOS, we can figure out absorption, the inverse of gain, by the following equation:

$$\alpha(\hbar\omega)=\alpha_0(\hbar\omega)[f_v(k_0)-f_c(k_0)] \tag{1.24}$$

where α_0 represents the absorption spectrum at thermal equilibrium, and f_c and f_v represent how much of conduction or valence band is occupied with carrier. Expressions are the following:

$$\alpha_0=C_0\,|\,\hat{e}\bullet p_{cv}\,|^2\;\rho_r(\hbar\omega-E_g) \tag{1.25}$$

$$k_0 = \sqrt{\frac{2m_r^*}{\hbar^2}(\hbar\omega - E_g)} \tag{1.26}$$

$$\frac{1}{m_r^*} = \frac{1}{m_e^*} + \frac{1}{m_h^*} \tag{1.27}$$

From Equation (1.24), we can see that when the diode is in quasi-Fermi level state, it will have two states, F_c and F_v, corresponding to electron and hole. They are represented by f_c and f_v, and when f_v - f_c is negative, which means that there are more carriers in conduction band than in valence band (called population inversion [1]), the absorption becomes negative, which is the same as gain. We can get these two equations from the description above:

$$e^{(E_c - F_c)/k_B T} < e^{(E_v - F_v)/k_B T} \tag{1.28}$$

$$F_c - F_v > E_c - E_v = \hbar\omega \tag{1.29}$$

1.4 Motivation and basics of narrow linewidth laser

There are many applications of lasers today, and some, like coherent optical communication, optical precision metrology, and high-resolution spectroscopy, require narrow linewidth. Also, there are other applications like fiber-optic sensors, interferometric sensing, and trace gas detection. Usually, the applications that require narrow linewidth are high-end technologies that need extremely small bandwidth to be precise and efficient.

There are a few types of narrow linewidth laser, and the two most commonly derived from the semiconductor laser are the DFB laser and DBR laser. Both structures use the change of the refractive index of the material and correct pitch and duty cycle, depending on emitted light wavelength, to reflect the single wavelength that is desired. Another way to get narrow linewidth from a semiconductor laser is to use an external cavity [17], a technique that employs a regular laser diode with anti-reflection coating on one side and high-reflection coating on the other. A

grating is placed in the path of the laser beam at the angle necessary to output the desired wavelength. H. Stoehr successfully demonstrated 1.5Hz linewidth in 2005 using this technique [18]. The other technique uses single-mode optical fiber with a fiber Bragg grating to extend the laser cavity. The physics behind fiber Bragg grating is similar to that behind DFB and DBR gratings. However, in a fiber Bragg grating, some materials are placed around the inner layer of the fiber at a certain pitch that determines the emitted wavelength rather than fabricating or modifying the laser structure [19].

To achieve narrow linewidth for the laser, there are a few essential factors that we need to consider. One is single-frequency operation. This can be achieved by using a gain medium with a small gain bandwidth and short-length laser resonator. Another factor is low noise. This means that we want to have minimum noise from external sources such as physical vibration of the laser diode, low-intensity noise for optical pump laser, and low-noise power supply that injects current or voltage for an electrically pumped laser. It is also important to eliminate optical feedback by using an isolator. Last, it is important to optimize the laser design for minimum phase noise. This can be done by making a long cavity or resonator, although a long cavity is detrimental to single-frequency operation.

CHAPTER 2. FABRICATION OF DBR LASER

Since the first fabricated semiconductor lasers [2-5], the quality of the crystal has been one of the important aspects that researchers have worked to improve by having fewer defects in the crystal. The crystal growth technique has been developed from liquid phase epitaxy (LPE) to metal-organic chemical vapor deposition (MOCVD) and molecular beam epitaxy (MBE). The fabricated laser in this thesis was made by MOCVD growth, which will be briefly discussed in section 2.1. The other important parts of the fabrication are etch solution, mask, etch time, handling and tools. However, they will vary depending on the design of the laser and the tools available, so this chapter describes the fabrication steps of the laser with tools available.

2.1 Laser structure growth on MOCVD

MOCVD is the most important part in laser design. It will determine the emitted wavelength of the laser, the amount of optical confinement and electrical confinement, and the transverse mode structure. Figure 2.1 illustrates the laser structure that I use for my 852nm laser diode.

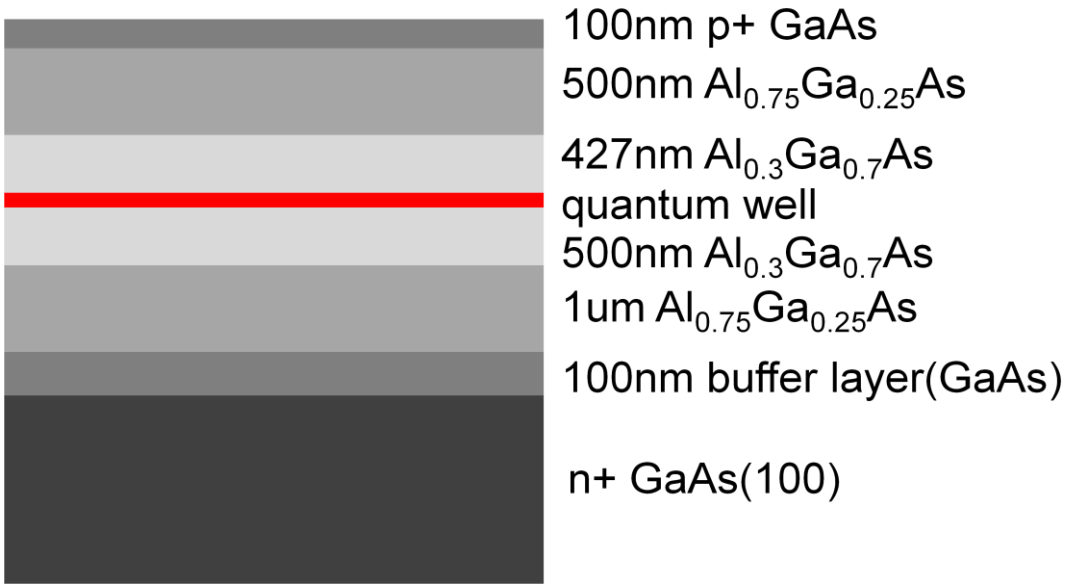

Fig 2.1 Epilayer structure for 852nm laser diode

The key factors of the emitted wavelength of the laser diode are the material and thickness of the quantum well, and we can calculate the emission wavelength with the Schrödinger equation [20].

$$\text{1D: } -\frac{\hbar^2}{2m}\frac{\partial^2\psi(z,t)}{\partial z^2}+V(z)\psi(z,t)=i\hbar\frac{\partial\psi(z,t)}{\partial t} \tag{2.1}$$

$$\text{3D: } -\frac{\hbar^2}{2m}\nabla^2\psi(z,t)+V(z)\psi(z,t)=i\hbar\frac{\partial\psi(z,t)}{\partial t} \tag{2.2}$$

where *m* represents the mass of the electrons or the holes of the element, *V* represents the barrier height or barrier difference between quantum well and the core material, and $\psi(z,t)$ represents the wave function of the particle. To calculate the emission wavelength of the laser, we need band-gap energy of the quantum well and the energy states that the electron and hole will occupy. We will assume that they will only occupy up to first states on each band because even though there will be some band filling in other states, there will be less overlap between other energy states than overlap between the lowest states of the conduction and valence bands. We can use the 1D Schrödinger equation and finite barrier model to calculate the first energy state of the conduction and valence bands. After that, we can use the simple calculation below to get the emission wavelength:

$$E_g + E_{n1} + E_{h1} = \frac{hc}{\lambda} \tag{2.3}$$

The other task is to structure the single transverse mode based on the difference in the refractive index of the different layers. It is usually the case that the material with smaller band-gap has higher refractive index and larger band-gap material has lower refractive index [21]. Therefore, the junction between two layers automatically functions as a waveguide of the laser

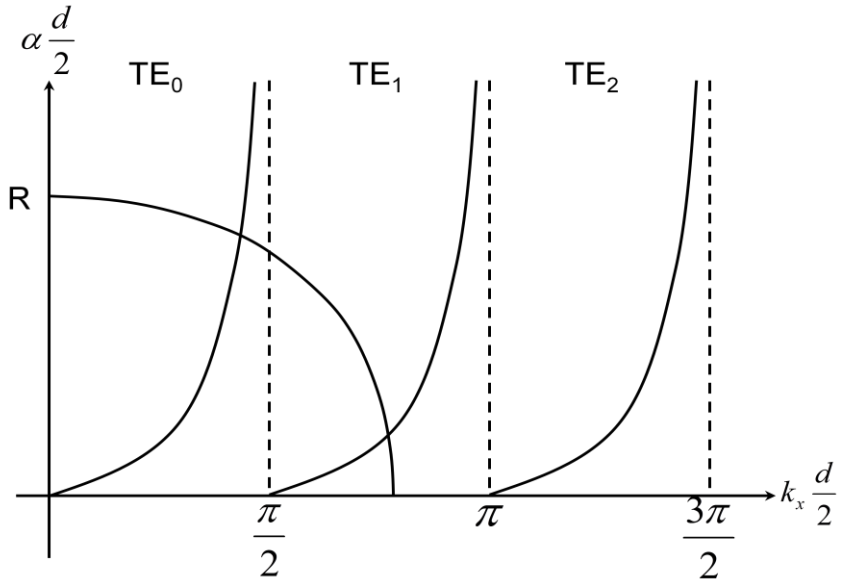

Fig 2.2 Graphical solution for guidance conditions

light. The equation for the waveguide is similar to the finite barrier model, and Figure 2.2 is the graphical solution for the guidance condition.

$$R = k_0 \frac{d}{2} (n_1^2 - n^2)^{1/2} \tag{2.4}$$

$$R^2 = X^2 + Y^2 \tag{2.5}$$

$$Y = \frac{\mu}{\mu_1} X \tan(X) \qquad \text{TE even modes} \tag{2.6}$$

$$Y = -\frac{\mu}{\mu_1} X \cot(X) \qquad \text{TE odd modes} \tag{2.7}$$

where R is the radius that is formed by the radius calculation of X and Y, k_0 is the wave number for the laser emission wavelength, μ is permeability of the material, d is the thickness of the quantum well or the medium through which the wave will propagate, and n_1 and n are the refractive indexes of the quantum well and the core material. R is the key factor to decide the single transverse mode laser by limiting R to be less than or equal to $\frac{\pi}{2}$. Therefore, with the

layer structure design, we can achieve a single transverse mode and decide the emission wavelength that we want.

2.2 Fabrication of broad area laser

The broad area laser is the basic laser that is used to check the wavelength of the epilayer structure because it is the simplest fabrication method for a laser. Also, this laser can be used in high power diode lasers because it is easy to achieve high power by alleviating power density of the facet by broadening the facet to prevent the facet degradation in high power. There is no exact definition or dimension to define the broad area laser, but it has a stripe geometry that guides the injected current to a certain region of the laser to get the gain and to have optical mode confinement in lateral direction. Therefore, it usually has a spatial and longitudinal multimode operation. There are two types of geometry that can be used. One is the etched p-cap layer geometry to define the current path, and the other is an oxide cap on top of the p-cap layer to define the current path. Figures 2.3 and 2.4 illustrate the geometry of the broad laser diode for each case.

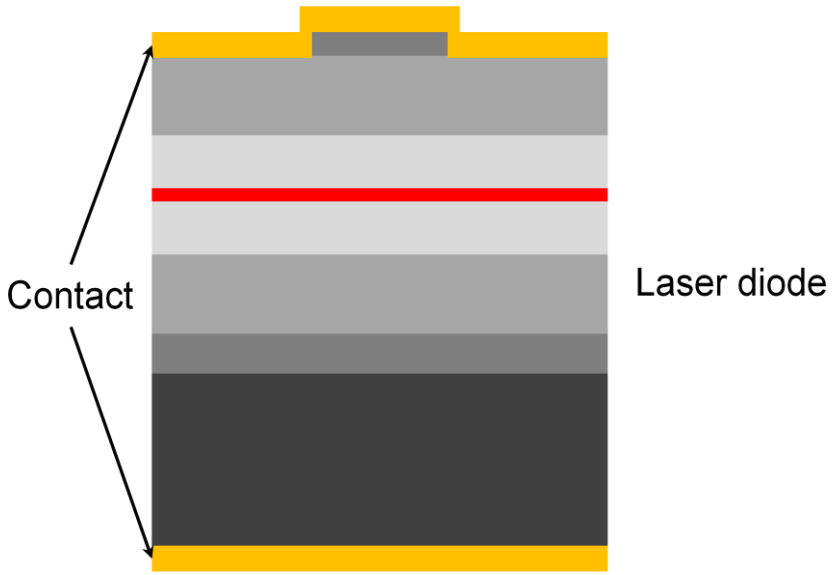

Fig 2.3 Etched p-cap layer geometry

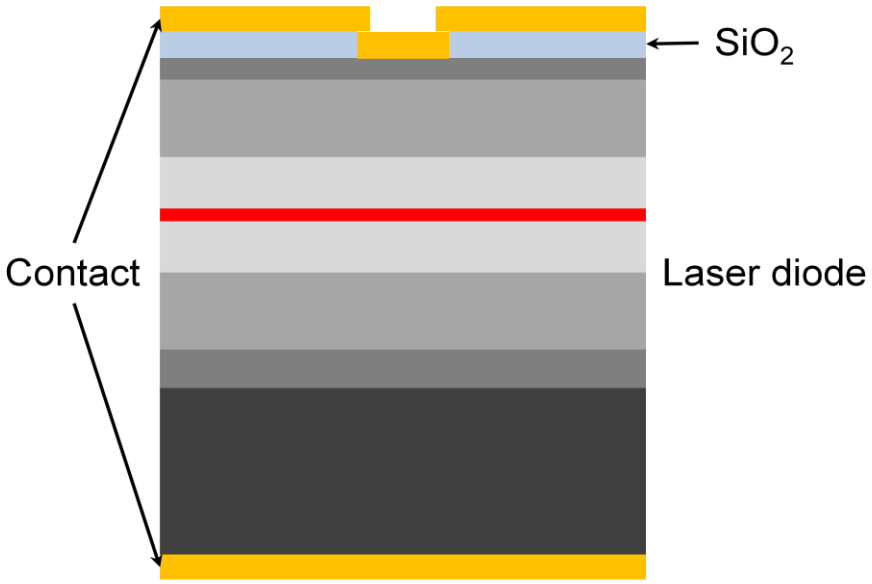

Fig 2.4 Oxide cap geometry

The difference between the two geometries is clearly shown in Figures 2.3 and 2.4. The etched p-cap geometry defines the path by removing the p+ GaAs down to the AlGaAs layer with citric acid with certain dimension, and the contact is put on top of that. Due to high contact resistivity of the AlGaAs and low contact resistivity of GaAs, when we inject the current through the top contact, it will only go through the p-cap GaAs layer region, which will limit the spread of the current through the laser diode and can confine the optical gain layer. The oxide cap geometry is a little bit different. Instead of etching down the p-cap layer of GaAs, it has an oxide layer on top of the p-cap layer with a window on a part of the oxide layer, and a contact on top of the oxide layer. The current will only go through the open part of the oxide layer because oxide is non-conductive, and that will confine the injected current to the central region to achieve the optical confinement.

Even though there are two ways to make a broad area laser, I used the etched p-cap layer geometry. The way I fabricate the etched p-cap layer is as follows: First apply HMDS and spin at 4500rpm for 30 seconds. After that, apply AZ5214 and spin it at 4500rpm for 30 seconds. After

flattening out PR by spinning, place the sample on a 110°C hot plate for 60 seconds for soft bake, and put into Karl Suss MJB3 with a stripe mask and expose it for 60 seconds. Develop the sample with AZ327 MIF developer for 55~70 seconds. After developing, dip the sample into the mixture of citric acid and hydrogen peroxide with the ratio of 20ml:5ml for 50~60 seconds to etch down to the AlGaAs layer. The PR should be removed after etch, so we dip the sample into acetone for 5 minutes and another 5 minutes with acetone, and 2 minutes of methanol and isopropyl alcohol (IPA), a process that is called 5-5-2-2. Even though acetone, methanol and IPA can remove PR, they cannot remove PR completely, so 3 minutes of O_2 descum should be done after the acetone-methanol-IPA. After PR removal, we can now do contact metal deposition on the top surface of the sample with 50nm of Ti, 100nm of Pt, and 100nm of Au by e-beam metal deposition. At this point, the laser diode is too thick to be cleaved easily. Therefore, the diode needs to be lapped and polished with grinding powder down to 5~6 mil. After lap and polish, we can deposit n-type metal with 5nm Ni, 80nm Ge-Au (88%, 12%), 30nm Ni, and 50nm Au. After depositing n-metal, it needs to be annealed to make ohmic contacts, and this should be done in H_2 environment at 425 °C until the gold color changes to silver due to the metal alloy. After this step, we can cleave and dice the laser diode and then test them.

2.3 Fabrication of ridge waveguide laser

The difference between ridge waveguide laser and broad area laser is that the ridge waveguide will have lower threshold current and narrow linewidth compared to a broad area laser. However, it also has the disadvantage of power limitation due to facet damage in high power since it has smaller light emission area that causes lower critical output power. The geometrical difference between ridge waveguide and broad area laser is the size of the current path from the top contact, as illustrated in Figure 2.5. Therefore, by designing a small current

path, one can achieve a better quality, more coherent laser beam than a broad area laser since the gain of a material by the current injection will be achieved only in the region where current passes through. However, the fabrication is a little bit more complicated than broad area laser because to make a sharp ridge for a ridge waveguide laser, we need to use dry etching instead of wet etching due to undercutting and isotropic etch characteristic. Also, I use the oxide cap method for the ridge waveguide laser. The first step is to deposit 100nm SiO_2 on top of the sample using PECVD, and apply HMDS and spin the sample at 4000rpm for 30 seconds, and repeat the same steps for PR. After PR coating, we put the sample on a 110°C hot plate for 60 seconds for soft bake, and expose with the ridge waveguide mask for 60 seconds. After exposure, we develop the sample with AZ327 MIF for 2 minutes. When the PR is fully developed, we use Freon RIE dry etching tool with CFH_3 gas and etch for 7.3 minutes to etch away SiO_2. When dry etching is completed, we do 5-5-2-2 to take the PR from the sample with an O_2 descum for 3 minutes. After removing PR, we need to use an inductively coupled plasma reactive ion etching (ICP RIE) dry etching tool to etch the GaAs cap layer down to the AlGaAs layer, but it is important to decide how deep we want to etch to make a single lateral mode laser. If we etch

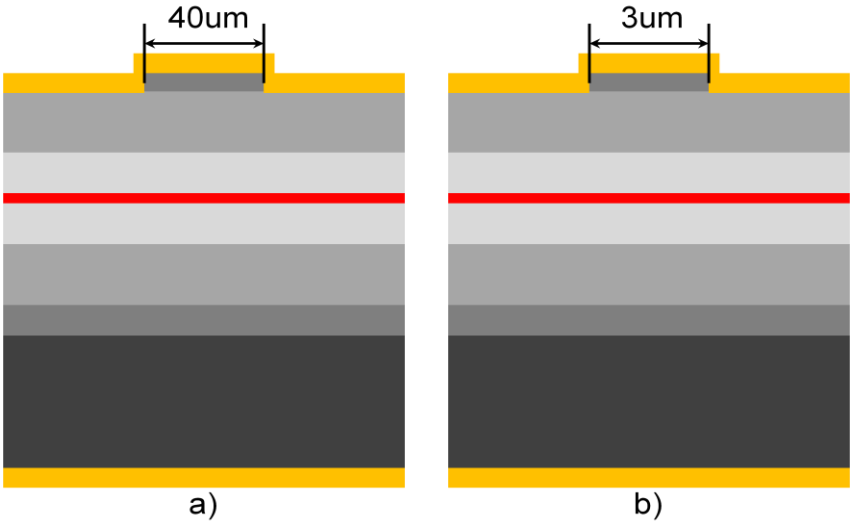

Fig 2.5 a) Broad area laser geometry, b) ridge waveguide laser geometry

down too deep, the device will not operate with a single lateral mode due to single lateral mode condition derived from waveguide theory, and the limit for single lateral mode is about 250nm deep for our structure. After ICP RIE etch, we need to do another Freon RIE etch for 5 minutes with CH_4 to remove the oxide mask. After that, we put SiO_2 using PECVD for the oxide cap layer, and dry etch again with thinner ridge waveguide mask with the same lithography step as before. When the lithography is finished, we will deposit p-contact with 50nm Ti, 100nm Pt, 100nm Au, and lap and polish the sample. After lap and polish, deposit N-contact with 5nm Ni, 80nm Ge-Au, 30nm Ni, 50nm Au, and anneal it at 425°C until color changes to silver around the whole surface. Figure 2.6 shows the geometry of a ridge waveguide laser.

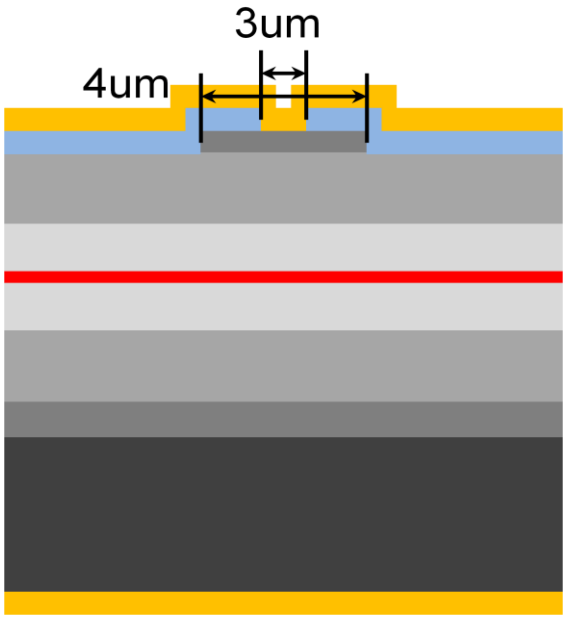

Fig 2.6 Ridge waveguide geometry

2.4 Fabrication of DBR laser

Making a DBR laser is not much different from making a broad area or ridge waveguide laser. The only difference is that there are a few extra steps on top of the regular laser fabrication to make the distributed Bragg reflector. Before going into detail about fabrication of the DBR

laser, I will briefly discuss the theory of DBR. DBR is simply alternating two materials with different refractive indexes back to back with a certain period in an array to pick the reflecting wavelength. (See Figure 2.7.)

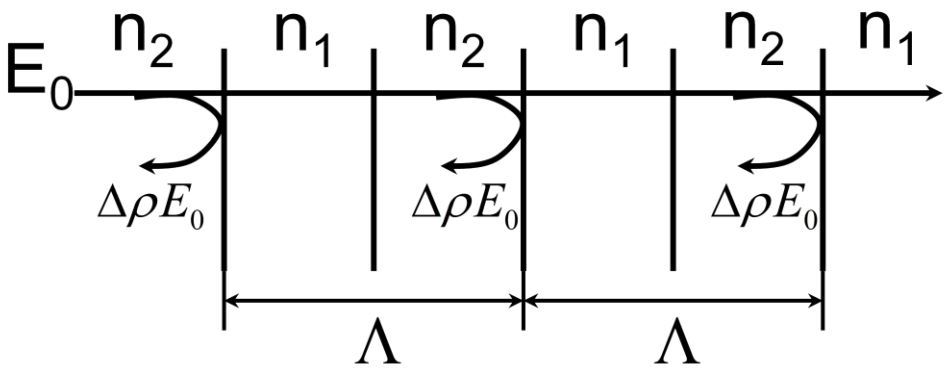

Fig 2.7 Schematic of multiple reflections for DBR grating

The sum of all the reflected waves is [13]

$$E = \Delta\rho E_0 e^{(-j0)} + \Delta\rho E_0 e^{(-jk2\Lambda)} + \Delta\rho E_0 e^{(-jk4\Lambda)} + ... \quad (2.8)$$

$\Delta\rho$ is the fraction of reflected wave from the total wave. To make a constructive reflection wave which makes it possible to pick a single wavelength, the following condition must be satisfied:

$$2k\Lambda = 2m\pi \quad (2.9)$$

$$\Lambda = \frac{m\lambda}{2n_{eff}} \quad (2.10)$$

Here, $k = \frac{2\pi}{\lambda}$, m is the order of grating, and n_{eff} is the effective refractive index of the laser structure. With this schematic, we can pick how wide a pitch we should make, but there is another factor that we need to consider: the duty cycle of the pitch, which is decided by the coupling coefficient κ. The coupling coefficient is the number that describes how much interaction there is between forward and backward propagating waves within a periodic structure like a DBR, and it is good to have a high coupling coefficient in order to get high reflectivity.

The equation below and the graph in Figure 2.8 correspond to the coupling coefficient with different duty cycle.

$$\kappa = \frac{w}{4}\int_{-\infty}^{\infty} \Delta n(x)\left|E(x)\right|^2 dx \tag{2.11}$$

Fig 2.8 Coupling coefficient vs. duty cycle with different order of grating

In equation 2.11, $\Delta n(x)$ represents the Fourier series expansion of the DBR grating periodic change in the refractive index, and $E(x)$ is the electromagnetic wave that goes through the DBR grating. As we can see from the simulated result, different grating orders should have different duty cycles to get the highest reflectivity.

Another physical concept that we need to use to calculate DBR is the "transmission matrix method" [13]. It describes the relationship between forward and backward propagating waves. We can set the whole system like the schematic in Figure 2.9.

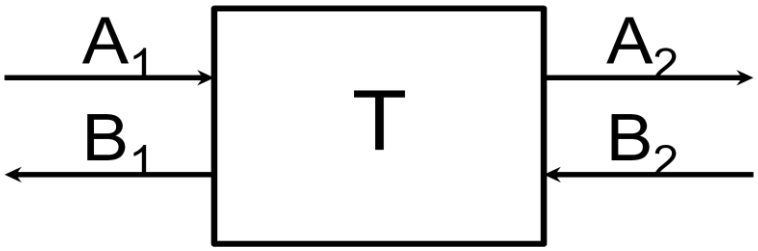

Fig 2.9 Two parts system with inputs and outputs

From the figure, we can set up two equations,

$$A_1 = T_{11}A_2 + T_{12}B_2 \tag{2.12}$$

$$B_1 = T_{21}A_2 + T_{22}B_2 \tag{2.13}$$

For propagation, we will assume that it is lossless for the simplification, and we can set the propagating medium to have the length, *L*, and make this relationship:

$$A_2 = A_1 e^{j\beta L} \tag{2.14}$$

$$B_1 = B_2 e^{j\beta L} \tag{2.15}$$

With the four equations above, we can convert them into transmitting dielectric matrix form:

$$T_{dielectric} = \begin{bmatrix} e^{-j\beta L} & 0 \\ 0 & e^{j\beta L} \end{bmatrix} \tag{2.16}$$

We also need to account for the reflection between two different media that can be calculated:

$$r_{12} = \frac{n_1 - n_2}{n_1 + n_2} = -r_{21} \tag{2.17}$$

The summation of the reflected wave and the transmitted wave should be the same as the initial wave, and that will be defined as

$$r^2 + t^2 = 1 \tag{2.18}$$

From the above equations, we can derive the following:

$$A_2 = t_{12}A_1 + r_{21}B_2 \tag{2.19}$$

$$B_1 = r_{12}A_1 + t_{21}B_2 \tag{2.20}$$

and Equations (2.19) and (2.20) can be converted to the same form as Equations (2.12) and (2.13):

$$A_1 = \frac{A_2}{t_{12}} - \frac{r_{21}B_2}{t_{12}} \tag{2.21}$$

$$B_1 = \frac{r_{12}A_2}{t_{12}} + \frac{B_2}{t_{12}} \tag{2.22}$$

We can express the above equations in the reflection matrix form as

$$T = \frac{1}{t_{12}}\begin{bmatrix} 1 & r_{12} \\ r_{12} & 1 \end{bmatrix} \tag{2.23}$$

Therefore, by multiplying both the transmitting dielectric matrix and reflection matrix, we can get one-way propagation from one material to the other, but the complete system is the propagation back and forth, so the calculation should be done twice in a different order than previous calculation, and it comes out as:

$$T_{total} = \frac{1}{t_{12}t_{21}}\begin{bmatrix} e^{-j\beta_1 L} & 0 \\ 0 & e^{j\beta_1 L} \end{bmatrix}\begin{bmatrix} 1 & r_{12} \\ r_{12} & 1 \end{bmatrix}\begin{bmatrix} e^{-j\beta_2 L} & 0 \\ 0 & e^{j\beta_2 L} \end{bmatrix}\begin{bmatrix} 1 & r_{21} \\ r_{21} & 1 \end{bmatrix} \tag{2.24}$$

The above equation is the expression for a single pair DBR grating, and we will have N pairs of this grating, so the expression can be finalized as:

$$T_{total} = \left(\frac{1}{t_{12}t_{21}}\begin{bmatrix} e^{-j\beta_1 L} & 0 \\ 0 & e^{j\beta_1 L} \end{bmatrix}\begin{bmatrix} 1 & r_{12} \\ r_{12} & 1 \end{bmatrix}\begin{bmatrix} e^{-j\beta_2 L} & 0 \\ 0 & e^{j\beta_2 L} \end{bmatrix}\begin{bmatrix} 1 & r_{21} \\ r_{21} & 1 \end{bmatrix} \right)^N \tag{2.25}$$

From this system in Figure 2.9, we can set the reflection of the wave in this system as:

$$r_{total} = \frac{B_1}{A_1} \tag{2.26}$$

Plugging Equation (2.25) into (2.26), we get:

$$r_{total} = \frac{T_{total21}A_2 + T_{total22}B_2}{T_{total11}A_2 + T_{total12}B_2} \tag{2.27}$$

We set the condition that there will be no input from the right-hand side, which sets B_2=0. That will conclude to:

$$r_{total} = \frac{T_{total21}}{T_{total11}} \tag{2.28}$$

Having discussed the physics behind the DBR grating, I now discuss the fabrication. First, we deposit 200nm of SiO_2 with PECVD. This oxide layer will be used as a mask in ICP RIE when we are making some gratings on the sample. After the oxide layer, we apply HMDS and spin the sample for 30 seconds at 3000rpm, and repeat the same procedure with PR. We place the sample on a hot plate at 110°C for 60 seconds, and use the alignment mark mask to expose the sample for 30 seconds. After exposure, we bake the sample on a 110°C hot plate for 45 seconds, and then expose the sample without mask on the aligner (flood exposure). This process is called negative lithography. After negative lithography, we put the sample into AZ 327 MIF developer for 70 seconds and look through a microscope to make sure that the opening of the alignment mark is clearly opened. If it is not fully opened, we dip it into the developer for a little longer and check again, and if it is not properly developed, we strip off PR and redo the negative lithography. When the opening for the alignment mark is clear, deposit 10nm of Ti, and 150nm of Au, so the mark can be observed with the JEOL (e-beam lithography equipment). Figure 2.10 is an SEM image of the alignment mark. The white cross in the image is where Ti and Au are deposited and the gray part is SiO_2. The cross mark is 6 μm thick, and it is 250 μm long horizontally and vertically.

The alignment mark is very important in ebeam lithography because if it is tilted too much or is unclear, it will be misexposed in the JEOL due to the equipment's precision error. After checking the alignment mark, we place the sample on a 200°C hot plate for 2 minutes for pre-baking. We apply 3% PMMA with 3000rpm spin for 60 seconds, re-bake the sample at 200°C for another 2 minutes, and load the sample on to JEOL and expose the sample. After exposure, we develop the sample with MLBK:IPA(1:2) mixture for 60 seconds and place into IPA for 30 seconds for rinse. We use CHF_3 Freon RIE for 17.6 minutes to etch away SiO_2 to pattern the

grating, and do 5-5-2-2 to take off PMMA, and O_2 descum. After cleaning PMMA, we inspect the sample with SEM to measure the pitch and duty cycle of the grating. Also, it is hard to get the correct pitch and duty cycle the first time because the equipment is sensitive and the pattern is small. Therefore, some test runs (dose test) are necessary before exposing the real pattern (see Figure 2.11). From Figure 2.11, the light gray represents SiO_2 on the sample, and dark gray represents the surface of the GaAs layer, so we can see that it is developed and etched properly with the right dose that makes almost 50% duty cycle. After a real exposure of the grating, we also need to make an etching test sample on the side to check the etching rate of ICP RIE (etch test). With an etch test, we can get the precise etching rate, so we can have a precise control of the etching depth of the grating which is critical in a single mode emission. When ICP RIE is completed, a CF_4 Freon RIE etch is needed to remove the oxide mask from the sample. After this step, we can decide to make either broad area DBR lasers, or ridge waveguide DBR lasers, and the steps will be the same. However, the only difference is that we will need to align the laser pattern on the mask with the DBR grating that is already on the sample, so it can have the DBR grating on the laser.

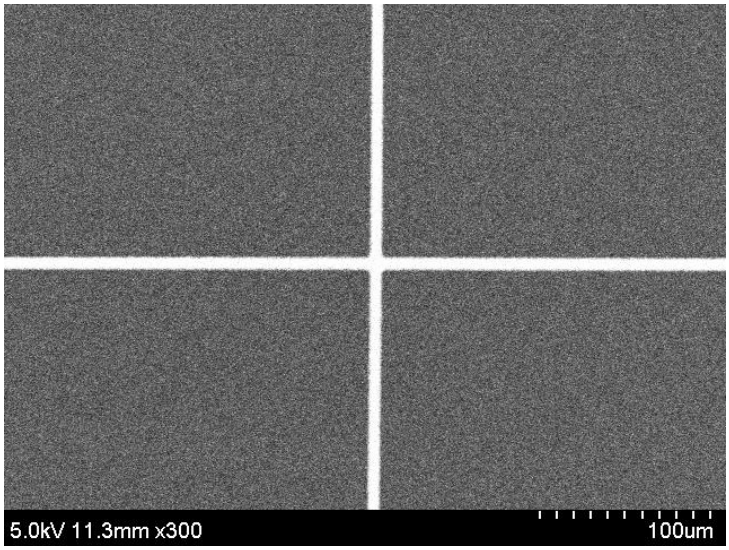

Fig 2.10 Alignment mark for ebeam

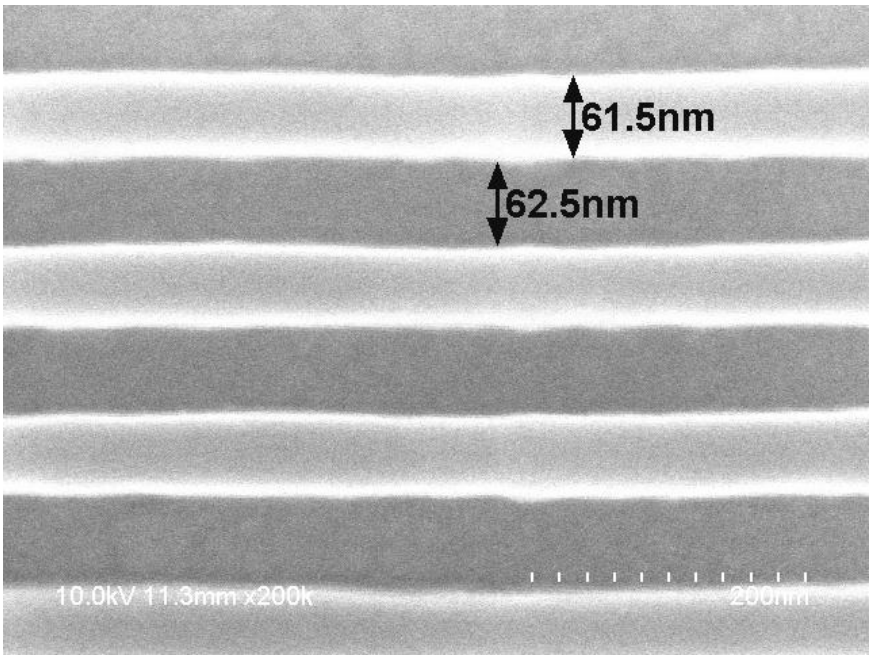

Fig 2.11 SEM image of grating

CHAPTER 3. TEST AND MEASUREMENT

After we fabricate the laser, it is also very important to test it. Even a laser designed for a specific wavelength still has a lot of variables that may change the emitting wavelength. Also, each individual diode may have slightly different characteristics and some are defective such that they may not perform as well as other lasers in the same batch. Common tests for a laser include measuring its wavelength, L-I-V testing for measuring the power of the emitted light as well as the power consumption of the laser, far field pattern measurement for divergence and beam profile of the light, and the linewidth which is the spectral linewidth of the laser. These four are the most common measurements for characterizing lasers.

3.1 Measurement of wavelength

When we make the laser, there is always a specific desired wavelength depending on the laser's purpose. For example, the laser that we are using for optical communication is either 1300nm or 1550nm because those two wavelengths have the best efficiency or the least loss when they go through the optical fiber. However, for storage devices like DVD or Blu-ray, we do not want a long wavelength because it decreases the amount of data that can be saved in a limited space. Therefore, it is important to know where the laser will be used before we design it, and after making the laser, it is critical to check the real emitted wavelength. To measure wavelength, researchers use many different tools with two schematics and either of the techniques schematized in Figure 3.1 and 3.2. The first method is to use a prism to separate the incoming light into many different wavelengths. Separation of the light can be figured from Snell's law:

$$n_1 k_0 \sin(\theta_1) = n_2 k_0 \sin(\theta_2) \tag{3.1}$$

where n_1 and n_2 correspond to the refractive indexes of the two different materials, air and the material of prism, and k_0 is the wave number with its wavelength, and θ_1 and θ_2 are the incident angle and the transmitted angle of the light.

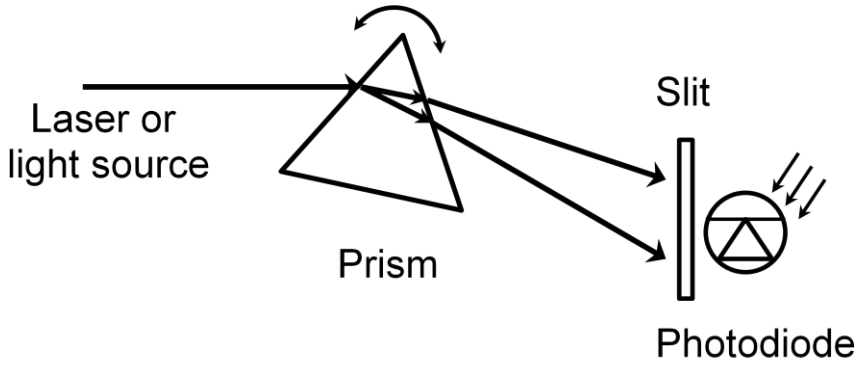

Fig 3.1 Separate the light using prism

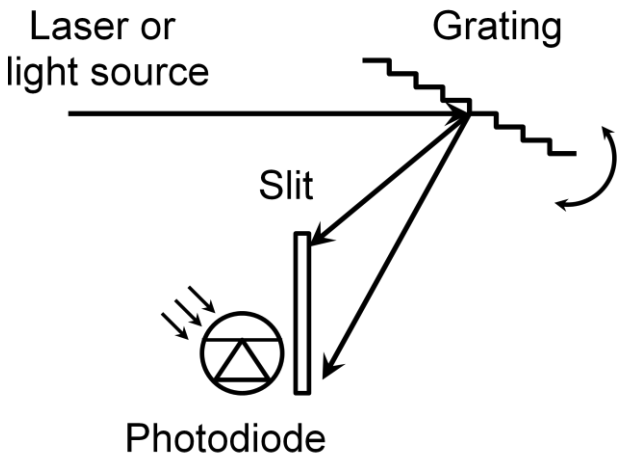

Fig 3.2 Separate the light using grating

When different wavelengths of light come into a prism, they all have the same refractive index, but they will have different wave numbers, causing differences in θ_2. Therefore, each wavelength will have a unique transmitted angle, making the separation of the light. An optical spectrum analyzer uses this physics by putting a photodiode with a slit at the fixed position, and this photodiode will detect the light. It is already calculated with Snell's law that the light with a specific wavelength will refract to the photodiode, and by rotating the prism, the photodiode will

detect the light with a different wavelength. The other method is to use the grating instead of a prism to diffract and reflect the light. This grating is called a blazed grating, and it diffracts as well as reflects the light. By using this grating, it is much faster and more space efficient to build an optical spectrum analyzer. For our setup, we use a multi-mode optical fiber with a proper lens mount that focuses the laser light to the opening of the optical fiber, and the optical fiber is connected directly to the optical spectrum analyzer to analyze the light.

3.2 Measurement of L-I-V curve

The second measurement that is essential in laser characterization is the L-I-V curve. L in L-I-V curve is for the light power that is emitted from the laser with the unit of intensity of the light, and I represents the injected current to the laser diode. V is the voltage across the laser diode. Therefore, with I and V, we can calculate how much power the laser diode requires, and with L, we can see how much power is converted to light from the laser diode. As low power or high efficiency is the future for engineering and technology, it is essential to have high efficiency for the laser, and some applications that require high power consider the efficiency to be very important because the cost of operating a high power laser will vary a lot with its efficiency. Another reason for measuring V is to see the mode hop of the laser, or in certain applications, to get a dynamic resistance curve (dV/dI) to make an equivalent circuit model using the IdV/dI curve. There are two modes in L-I-V testing: pulsed and continuous wave. Pulsed mode test only measures L-I because it is just used to see the operation of the laser as functional or not. The reason is that it does not need any heat sink or temperature control device such as a thermoelectric coolant, so it is much easier and more convenient to check the behavior of the laser and check for operation. Also, the power calculation is not accurate for pulsed mode due to its pulsed behavior that has some delay in pulsed signal. Continuous wave mode test requires a

heat sink or a thermoelectric coolant because the series resistance of the laser will generate heat that causes shifting in the emission wavelength or catastrophic optical damage (facet damage) which is irreparable. Measuring the light intensity requires a few pieces of equipment. First is an integrated sphere. It has two holes, one for the entrance of the light and the other for the exit, so the light can come into the entrance, reflect inside the integrated sphere and go out the exit. The reason for using this equipment is to collect as much light as possible that comes out of the laser because the laser has a huge divergence that makes it hard to measure its total light power. The second piece of equipment is a detector. The detector will vary depending on the emission wavelength of the laser because different detectors have different detecting wavelengths. Three detectors are most commonly used: silicon, germanium, and indium gallium arsenide. A silicon detector usually has a detecting wavelength from 300nm to 1100nm, germanium from 800nm to 1800nm, and InGaAs from 1200nm to 2600nm. It is important to choose the correct detector that corresponds with the emission wavelength. Figure 3.3 illustrates the integrated sphere and photodetector. The final piece of equipment is either a voltage meter or a current meter that measures the current output from the photodetector, so we can measure how much power the photodiode absorbs from the laser.

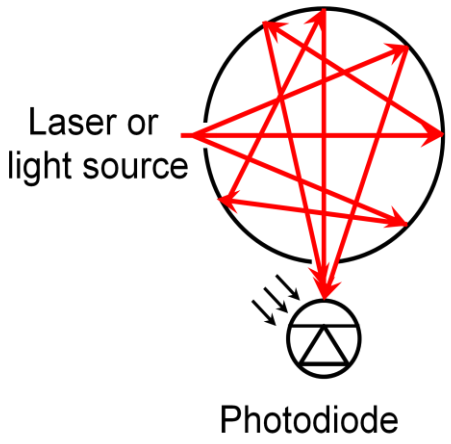

Fig 3.3 Laser with integrated sphere and photodetector

The L-I-V test setup does not require a current measurement tool because it usually uses a current source by which we can set the injected current, and we can just use that as the information for the current. The voltage is similar because the current source usually gives the voltage that it generates to make the current that the user asks for. Therefore, we can just use the value that a current generator shows as the voltage for V. With these three values, we can draw an L-I-V curve that looks like Figure 3.4, and we can figure out the input power and the output power (light power) to get the efficiency of the laser.

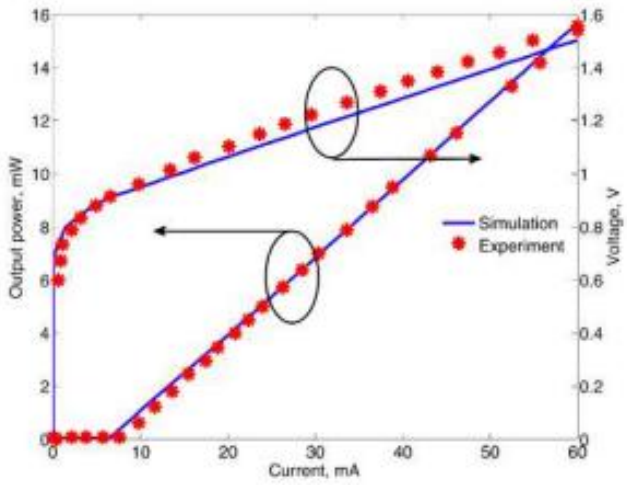

Fig 3.4 L-I-V curve [22]

3.3 Measurement of far field pattern and near field pattern

The measurement of the far field and near field patterns is the measurement of spatial coherence that tells us how circular the beam is. For example, a laser pointer has one point where all the light is focused, so many people think that a laser generates a small spot of light. However, the fact is that the light from the laser requires corrective optics to focus in a certain area. One must know the divergence angle of the light to have the correct optics to focus it properly, so far field and near field pattern measurement is to figure out the divergence angle of the light. The measurement of the near field pattern is straightforward. It requires a camera that

can capture the light coming out from the facet of the diode, so a correct photodetector is necessary. Another requirement is a microscope on which the camera can be mounted in order to capture the field of view of the microscope. After all this setup, proper mounting is required that can pump the laser facing the bottom optics of the microscope, so the camera can capture the image of the facet and where the light is emitted from the facet.

The other measurement is of the far field pattern, and it is more complicated because it requires some optics to focus the light properly at a great distance. This measurement requires some optics to focus the diverged light to keep its shape and shine the maximum amount of light into the photodetector. Figure 3.5 is the result of far field pattern measurement of a vertical cavity surface-emitting laser (VCSEL). It is clear how the laser beam changes shape at a certain distance with different currents, and we can observe the mode profile of the laser, too.

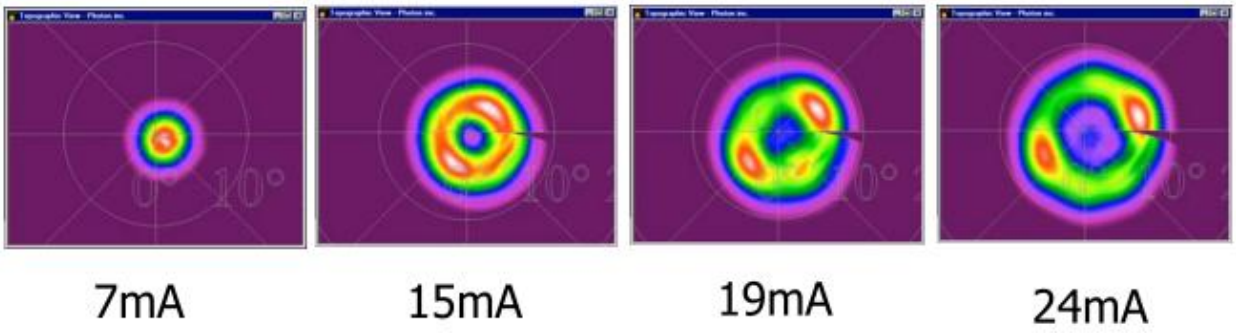

Fig 3.5 Far field pattern of VCSEL with different current [23]

3.4 Measurement of linewidth

The last measurement that I will discuss is the measurement of the linewidth. It may seem easy to measure the linewidth by using an optical spectrum analyzer, like when we measure the emission wavelength, but the problem is that it does not provide enough resolution to measure the linewidth of the laser. Therefore, a specific setup is required to measure the linewidth of the laser, and there are many theories and methods for doing this. These include the self-heterodyne

system, delayed self-heterodyne system, Fabry Perot interferometer, and self-homodyne system, and many other methods are still developing. This thesis discusses only the delayed-self-heterodyne system, illustrated in Figure 3.6.

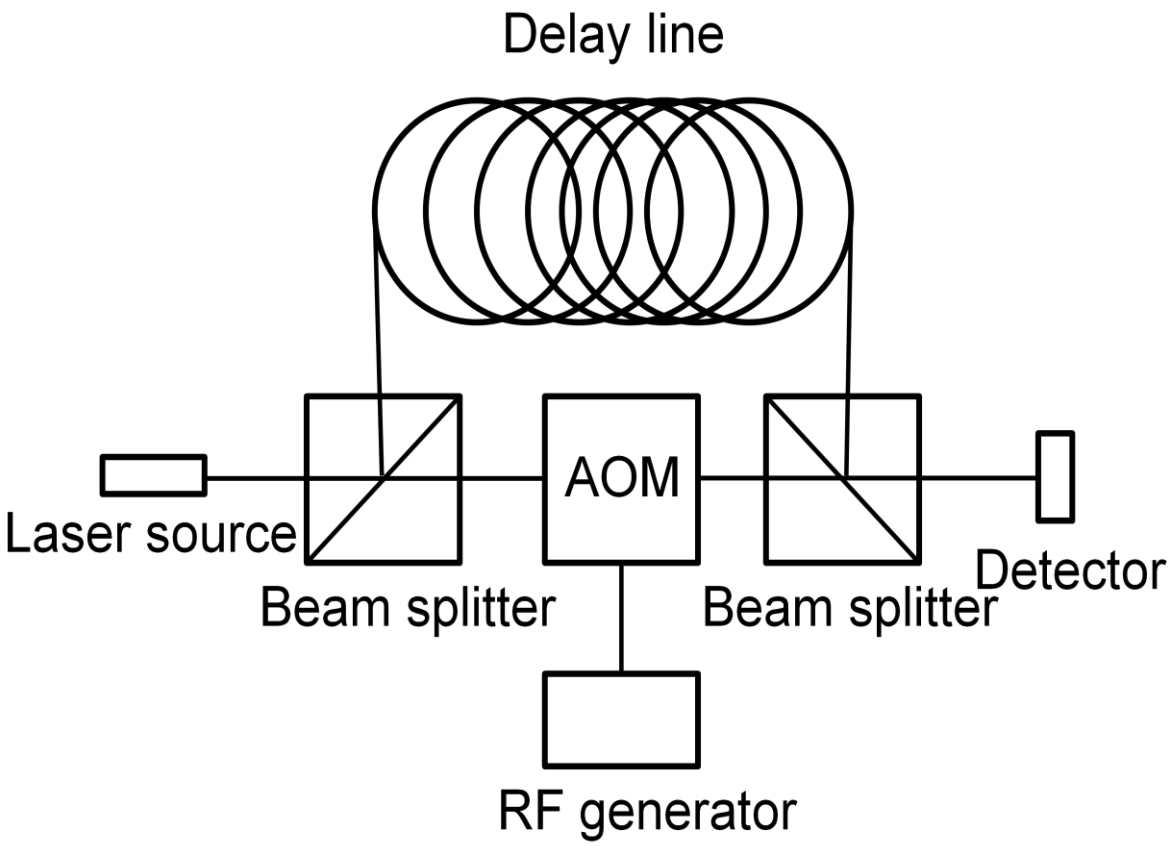

Fig 3.6 Delayed-self-heterodyne system

The heterodyne system has a single frequency laser source. The light source will go into the optical isolator to prevent its reflection into the laser that causes noise, and after the optical isolator, a beam splitter splits the beam into two beams of equal intensity. One beam goes into a delay line, and the other goes into an acousto-optic modulator (AOM) that shifts the optical frequency of the beam. The two beams converge in another beam splitter, and the combined beam goes into a fast photodetector from which an RF spectrum analyzer will get the signal. When we look at the signal of each part, as shown in Figure 3.7, it will be clear how it works.

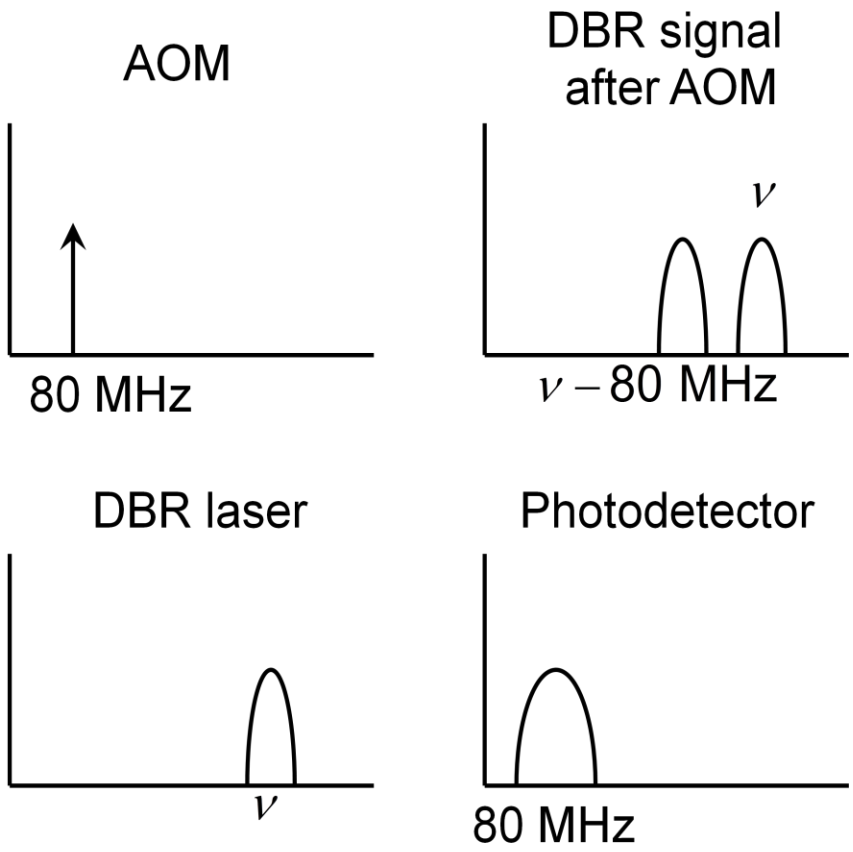

Fig 3.7 Signals at different positions of the heterodyne system

As we can see from the figure, when the beam goes through the AOM, it modulates the DBR signal down with RF generator frequency due to its convolution property. One assumption is that the signal generated by the RF generator is much narrower than the DBR signal, so it can be treated as a delta function. The other beam that goes into the delay line should be delayed longer than the coherence time of the laser; otherwise, it will correlate the delayed light and frequency-shifted light, making the analysis of the spectral linewidth harder. Therefore, a longer delay line that makes the delay longer than the coherence time of the laser will make two identical lights independent of each other. When the high speed photodetector detects the light, it will detect the signal with RF frequency, which will make an overlap of the two identical lights with different frequencies. This greatly eases the interpretation of the laser linewidth because it is

at the frequency where the RF spectrum analyzer can detect the signal. Otherwise, we need to have a very high-frequency spectrum analyzer to measure the linewidth of the laser, which is hard to make. The measurement linewidth of a laser is expected to be Lorentzian shape because of the random atomic state transition that occurs for emitting light which is derived as Lorentzian distribution in quantum mechanics. We can clearly see that the spectral shape of the linewidth is Lorentzian instead of Gaussian as it is shown in Figure 3.8, and the Lorentzian shape of the laser linewidth was calculated by Schawlow and Townes before it was demonstrated [24].

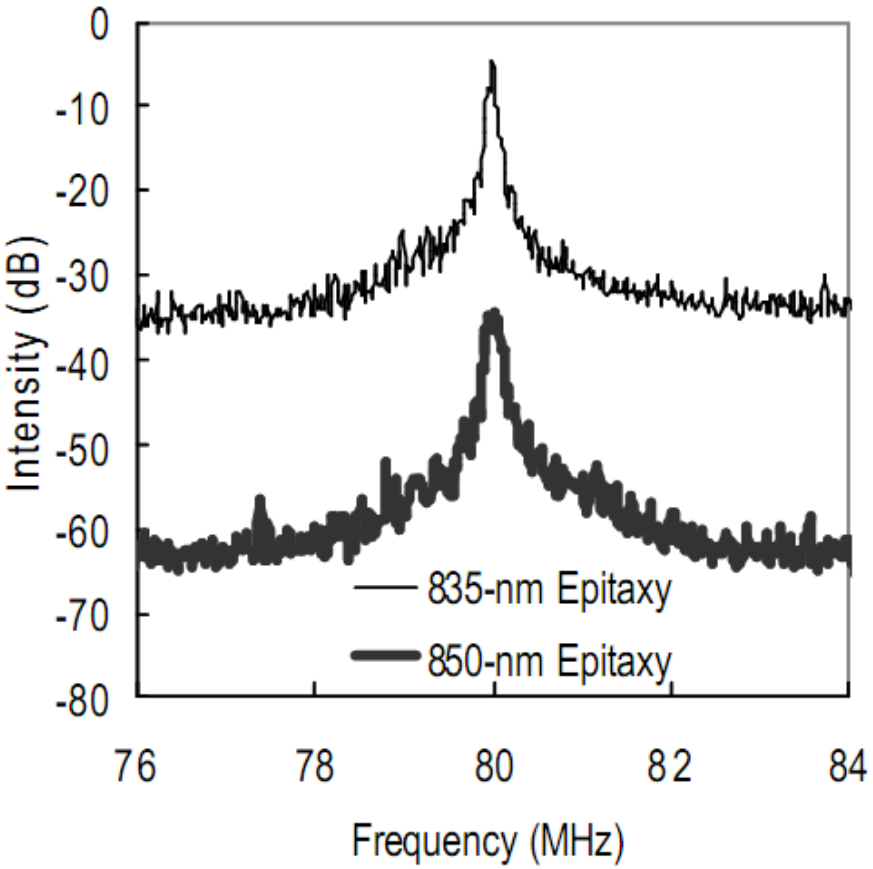

Fig 3.8 Minimum measured spectral linewidths for the 835nm and 850nm devices [25]

CHAPTER 4. CONCLUSION

This thesis summarized the basics of the semiconductor laser from the history of the semiconductor to the measurement of the semiconductor laser. There are many different types of laser with different applications, and this thesis is focused on the narrow linewidth laser. The semiconductor laser can be made to operate at all different wavelengths. The emission wavelength is decided by the gain material that is used in some types of confined dimension structures, and can be structured by metal-organic chemical vapor epitaxy (MOCVD). After we grow the laser structure on the wafer, the wafer is processed with a certain method depending on what type of laser it is. The lasers discussed in this thesis are broad area, ridge waveguide, and distributed Bragg reflector (DBR) lasers. DBR can be integrated with either broad area laser or ridge waveguide laser, and it is an essential process to achieve narrow linewidth. This thesis also discusses the four important characterizations of the laser: wavelength, L-I-V curve, far field and near field patterns, and linewidth. The wavelength is important because it is different depending on applications, and the L-I-V curve shows the laser's light output power, power consumption, dynamic resistance, and efficiency. Far field and near field patterns tell how the shape of the laser changes, and it is necessary to know the shape of the laser to design some of its optics. The last characterization is the linewidth of the laser. Many advanced technologies that require high resolution need to have the narrow linewidth laser, so it is important to measure and see how the linewidth changes with different injected currents and operating temperatures.

REFERENCES

[1] M. G. A Bernard and G. Duraffourg, "Laser conditions in semiconductors," *Phys. Stat. Solidi,* vol. 1, pp. 699-703, 1961.

[2] R. N. Hall, G. E. Fenner, J. D. Kingsley, T. J. Soltys, and R. O. Carlson, "Coherent light emission from GaAs junctions," *Phys. Rev. Lett.,* vol. 9, pp. 366-368, 1962.

[3] M. I. Nathan, W. P. Dunke, G. Burns, F. H. Dill, Jr., and G. Laher, "Stimulated emission of radiation from GaAs p-n junctions," *Appl. Phys. Lett.,* vol. 1, pp. 62-64, 1962.

[4] T. M. Quist, R. H. Rediker, R. J. Keyes, W. E. Krag, B. Lax, A. L. McWhorter, and H. J. Zeiger, "Semiconductor maser of GaAs," *Appl. Phys. Lett.,* vol. 1, pp. 91-92, 1962.

[5] N. Holonyak, Jr., and S. F. Bevacqua, "Coherent (visible) light emission from $Ga(As_{1-x}P_x)$ junctions," *Appl. Phys. Lett.,* vol. 1, pp. 82-83, 1962.

[6] M. H. Pilkuhn and H. S. Rupprecht, "Junction heating of GaAs Injection lasers during continuous operation," *IBM Journal*, vol. 9, no. 5/6 pp. 400-404, 1965.

[7] H. Kroemer, "A proposed class of heterojunction injections lasers," in *Proc. IEEE*, vol. 51, 1963, pp. 1782-1783.

[8] H. Kressel and H. Nelson, "Close-confinement gallium arsenide pn junction lasers with reduced optical loss at room temperature," *RCA rev,* vol. 30, pp. 106-113, 1969.

[9] I. Hayashi, M. B. Panish and P. W. Foy, "A low-threshold room-temperature injection laser," *IEEE J. Quant. Electron.,* vol. QE-5, pp. 211-212, 1969.

[10] I. Hayashi, M. Panish, P. Foy and S. Sumski, "Junction lasers which operate continuously at room temperature," *App. Phys. Lett.,* vol. 17, pp. 109-111, 1970.

[11] M.B. Panish *et al.,* "Reduction of threshold current density in GaAs $Al_xGa_{1-x}As$ heterostructure lasers by separate optical and carrier confinement," *App. Phys. Lett.,* vol. 22, pp. 590-591, 1973.

[12] R. Dingle, W. Wiegmann and C. Henry, "Quantum states of confined carriers in very thin $Al_xGa_{1-x}As$-GaAs-$Al_xGa_{1-x}As$ heterostructures," *Physical Review Letters,* vol. 33, pp. 827-830, 1974.

[13] D. Scifres, R. Burnham and W. Streifer, "Distributed-feedback single heterojunction GaAs diode laser," *Appl. Phys. Lett.,* vol. 25, pp. 203-206, 1974.

[14] F. Reinhart, R. Logan and C. V. Shank, "GaAs-$Al_xGa_{1-x}As$ injection lasers with distributed Bragg reflectors," *Appl. Phys. Lett.,* vol. 27, pp. 45-48, 1975.

[15] J. Kotik and M.C. Newstein, "Theory of LASER oscillations in Fabry-Perot resonators," *Appl. Phys. Lett.*, vol. 32, pp.178-186, 1961.

[16] S. L. Chuang, *Physics of Optoelectronic Devices*. New York, NY: Wiley & Sons, 2009.

[17] M. G. Litman and H. J. Metcalf, "Spectrally narrow pulsed dye laser without beam expander," *Applied Optics*, vol. 17, No. 14, pp. 2224-2227, 1978.

[18] H. Stoehr, F. Mensing, J. Helmcke, and U. Sterr, "Diode laser with 1 Hz linewidth," *Optics Letters*, vol. 31, no. 6, pp. 736-738, 2006

[19] K. O. Hill, Y. Fujii, D. C. Johnson, and B. S. Kawasaki, "Photosensitivity in optical fiber waveguides: Application to reflection filter fabrication," *Appl. Phys. Lett.*, vol. 32, pp. 647-649, 1978.

[20] E. Schrödinger, "An undulatory theory of the mechanics of atoms and molecules," *Physical Review*, vol. 28, No. 6, pp. 1049-1070, 1926.

[21] T. S. Moss, "A relationship between the refractive index and the infra-red threshold of sensitivity for photoconductors," *Proc. Phys. Soc. B.*, vol. 63, pp. 167-176, 1950.

[22] Z. Duan, W. Shi, L. Chrostowski, X. Huang, N. Zhou, and G. Chai, "Design and epitaxy of 1.5 um InGaAsP-InP MQW material for a transistor laser," *Optics Express*, vol. 18, No. 2, pp. 1501-1509, 2010.

[23] J. L. Guttman and J. M. Fleischer, "Characterization of the near-field profile of semiconductor lasers and the spot size of tightly focused laser beams from far-field measurements," *7th International Workshop on Laser Beam and Optics Characterization*, Sept 18-19, pp. 17, 2002.

[24] A. L. Schawlow and C. H. Townes, "Infrared and optical masers," *Physical Review*, vol. 112, No. 6, pp. 1940-1949, 1958.

[25] R. K. Price, "Surface-Etched distributed Bragg reflector lasers in photonic integrated circuits," *Ph. D thesis*, pp75, 2007.